

Structural analysis of the La Colorada Mine, Sonora, Mexico

Ricardo Vega-Granillo^{1*}, Víctor Hugo Vázquez-Armenta¹, Alberto Orozco-Garza², and Jesús Roberto Vidal-Solano¹

¹Departamento de Geología, Universidad de Sonora Apdo., Postal 847, 83000 Hermosillo, Sonora, Mexico.

²Argonaut Gold Inc., 83148 Hermosillo, Sonora, Mexico.

*rvega@ciencias.uson.mx

ABSTRACT

La Colorada Mine is an important gold and silver deposit located in the Sonora state, NW Mexico. Mineralization consists of quartz veins containing carbonates, sulphides, with silver and gold ore. The veins were emplaced along normal faults and related breccia zones. Our structural study recognizes one folding phase imposed on Paleozoic to Mesozoic (?) sedimentary rocks, which is ascribed to the Late Cretaceous Laramide Orogeny based on the orientation of the structures and the age of the units. Four sets of normal faults were recognized and its relative age defined based on crosscutting relationships, stratigraphy, rock ages, contacts, and structural analyses. The first set strikes ENE-WSW to E-W and dips both N and S. Faults of this set host the main mineralized veins, which have been dated between 27 and 22 Ma. The second set consists of NW-SE striking faults, with SW and NE dip. Similarly oriented structures occur in the Basin and Range physiographic province, which has been dated in Sonora between ~26 and 15 Ma. The third set is represented by a NE-SW striking conjugate fault system, which predates or is coeval to a widespread peralkaline ignimbrite dated at 12.3 Ma. The fourth set of conjugate faults strikes NNW-SSE and may have been active from 10 Ma to the present. These mid-late Tertiary fault sets suggest that changes in the stress field occurred from the final phase of subduction until the present.

Key words: Structural analysis; Tertiary extension; La Colorada mine; Sonora.

RESUMEN

La mina de La Colorada es un depósito importante de oro y plata localizado en el Estado de Sonora, NW de México. La mineralización consiste de vetas de cuarzo que contienen carbonatos, sulfuros, con una mena de oro y plata. Las vetas fueron emplazadas a lo largo de fallas normales y zonas de brecha relacionadas. El estudio estructural indica que al menos una fase de plegamiento afectó a rocas sedimentarias Paleozoicas y Mesozoicas (?). Esta fase de plegamiento se atribuye a la orogenia Laramide del Cretácico Tardío con base en la orientación de las estructuras y la edad de las rocas afectadas. Se reconocieron cuatro grupos de fallas normales y se estableció su edad relativa con base en sus relaciones de corte, estratigrafía, edad de las rocas, contactos y en el análisis estructural. El primer grupo tiene rumbos ENE-WSW a E-W y echados al N y al S. Las estructuras de esta fase encierran las principales venas mineralizadas del área, que fueron fechadas entre 27 y 22 Ma. El segundo grupo de fallas tiene rumbos NW-SE y echados al SW y NE.

Estructuras similares se produjeron en buena parte de Sonora entre ~26 y 15 Ma y generaron la provincia fisiográfica de cuencas y sierras paralelas. El tercer grupo de fallas conjugadas tiene rumbos NE-SW. Se considera que este grupo es anterior o contemporáneo al emplazamiento de una ignimbrita hiperalcalina datada en 12.3 Ma. El cuarto conjunto de fallas conjugadas tiene rumbos NNW-SSE. Esta fase pudo ocurrir entre 10 Ma y el presente. Las cuatro fases de fallamiento sugieren cambios en el campo de esfuerzos durante la fase final de la subducción hasta el presente.

Palabras clave: análisis estructural; extensión terciaria; mina La Colorada; Sonora.

INTRODUCTION

The La Colorada Mine is an important gold and silver deposit located in the Sonora state, northwestern Mexico. Mineralization occurs along fault controlled veins and related breccias. High-grade veins were intermittently mined through underground works from 1740 until 1993 when a large-scale mining operation began. A first stage of open-pit mining, from 1993 to 2000, produced three large pits named Gran Central, La Colorada, and El Crestón. Geology of the La Colorada region is described in some papers and technical reports *e.g.* Lewis *et al.* (1995), Zawada (1998), Zawada *et al.* (2001), McMillan and Hodder (2008), McMillan *et al.* (2009), which are devoted to explaining the history of the mining and the geology of the area, and to characterizing the ore deposits. Although the deposit is structurally controlled, few structural data have been reported apart from the attitude of the main ore veins and some major faults. In view of the expansion of the mining works, a better knowledge of the deposit is required and a detailed structural work was carried out, taking advantage of artificial outcrops in the open pits. Detailed structural data combined with field observations and structural analysis were used to define the main fault systems in the area, the relative age of faulting, as well as the role of the geological structures in the origin and later evolution of the ore deposits. Based on comparisons with adjacent areas, a model for the tectonic evolution in the area is proposed.

REGIONAL SETTING

The study area is located in the Cortés terrane near the border of the Caborca terrane (Figure 1). The Caborca terrane is made by Paleoproterozoic (1.8 to 1.7 Ga) metamorphic basement, intruded by ~1.4 and ~1.1 Ga granites (*e.g.* Anderson and Silver, 2005), covered

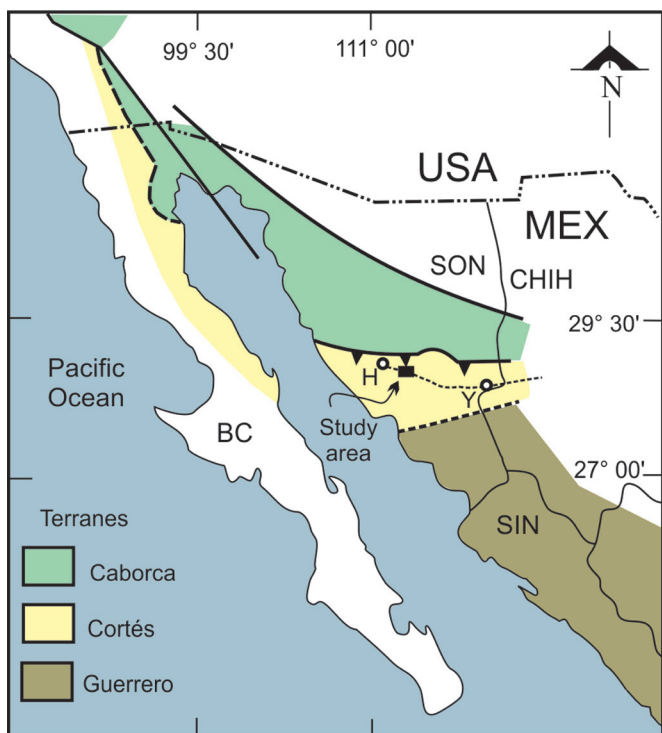


Figure 1. Location of the study area in a tectonostratigraphic terrane map. Countries: MEX = Mexico, USA = United States of America; States: BC = Baja California, CHIH = Chihuahua, SIN = Sinaloa; SON = Sonora. Towns: H = Hermosillo, Y = Yécora.

by a thick Upper Proterozoic to Lower Permian shelf succession (e.g. Stewart *et al.*, 1984). The Cortés terrane consists of Paleozoic deep-marine rocks deposited on thinned continental crust (Poole and Madrid, 1988; Coney and Campa, 1984), which was thrust over the Caborca terrane. This tectonic limit was described near of the Cobachi and Mazatán towns located about 40 and 60 km east of the study area, respectively (Ketner and Noll, 1987; Poole *et al.*, 1988). The Paleozoic allochthonous unit was covered in an angular unconformity by the Late Triassic-Lower Jurassic Barranca Group made up of sandstone, shale and conglomerate, with coal beds and tuffaceous layers (Radelli *et al.*, 1987; Stewart and Roldán-Quintana, 1991; Alencaster de Cserna, 1961; Weber *et al.*, 1980; Weber, 1995). The Barranca Group is interpreted to have been deposited in a rift-type basin, presumably bounded by ~E-W oriented faults (Stewart and Roldán-Quintana, 1991). Intermediate to felsic volcanic flows, tuff, and agglomerate, with minor interbedded continental sedimentary rocks, making up the Tarahumara Formation unconformably overlay the Barranca Group and the Paleozoic sequences. Volcanic rocks yielded ages between 90 and 70 Ma in Central Sonora (McDowell *et al.*, 2001), and of ~79 to 59 Ma in northeastern Sonora (González-León *et al.*, 2011). Large composite batholiths varying from diorite to alkaline granite (e.g., Roldán-Quintana, 1991; Valencia-Moreno *et al.*, 2001) were intruded between 90 and 40 Ma (e.g. Damon *et al.*, 1983; Ramos-Velázquez *et al.*, 2008; González-León *et al.*, 2011). A major pulse of Oligocene-Early Miocene silicic volcanism known as the Upper Volcanic Supergroup followed the Eocene magmatism (McDowell and Keizer, 1977). This pulse consisting of rhyolitic ignimbrites, air-fall tuffs, silicic to intermediate lavas, and lesser mafic lavas, yield K-Ar and Ar-Ar ages between 33 and 28 Ma (e.g. McDowell and Mauger, 1994; Albrecht and Goldstein, 2000; Gans, 1997). Basaltic andesites emplaced during and after the ignimbritic episode, known as the Southern Cordillera Basaltic

Andesites (SCORBA) yield ages between 33 and 17.6 Ma (Cameron *et al.*, 1989; McDowell *et al.*, 1997; Bartolini *et al.*, 1994; Paz-Moreno *et al.*, 2003), although most ages are Oligocene. Volcanic rocks of this pulse reach up to 1000 m in the Sierra Madre Occidental core but become significantly thinner toward the west (McDowell and Clubaugh, 1981). In the Sierra Santa Úrsula, located 70 km southwest of the study area, a volcanic sequence of ignimbrites, andesites, and dacitic domes yield ages between ca. 23 and 15 Ma (Mora-Álvarez and McDowell, 2000).

The tectonic regime in Sonora and large part of the Cordillera changed from Late Cretaceous-early Tertiary shortening to middle Tertiary extension (e.g. Calmus *et al.*, 2011), and then, to late Tertiary transtension related to the opening of the Gulf of California. This Tertiary tectonic regime produced major crustal extension, with the formation of low-angle faulting and associated metamorphic core complexes (MCC), as well as areas of more limited extension with high-angle normal faulting forming horst and graben or half-graben systems. The latter style of faulting was responsible of the formation of the Basin and Range physiographic province. Thick clastic sequences intercalated with minor basaltic to rhyolitic rocks filled both the MCC and Basin and Range basins. In the latter type of basins, these sequences are known as the Baucarit Formation (King, 1939; González-León *et al.*, 2011). Volcanic rocks underlying these continental sedimentary sequences have been dated at 27 Ma (Miranda-Gasca and De Jong, 1992; McDowell *et al.*, 1997; Gans, 1997). Volcanic rocks intercalated with clastic sequences yielded ages from ca. 25 to 18 Ma (e.g. McDowell *et al.*, 1997). Extension in the MCC and Basin and Range province of Sonora is constrained mainly between 25 and 15 Ma (Nourse *et al.*, 1994; Gans, 1997; Wong and Gans, 2008). The upper part of the graben-basin successions is less lithified and is intercalated with a distinctive Middle Miocene peralkaline ignimbrite dated at ~12.5 Ma (McDowell *et al.*, 1997; Vidal-Solano *et al.*, 2005, 2007). A post- ~10 Ma faulting phase causing tilting of the peralkaline ignimbrite and related rocks is inferred to accommodate modest amounts (~15%) of ENE-WSW extension in some areas (Gans, 1997).

LOCAL GEOLOGY

The older rocks in the area are informally named as “siliceous siltstone unit”, “transitional unit”, “quartzite unit”, “ribbon chert unit”, and “sandy dolomite unit” (Figures 2 and 3), from the structural base to the top. These units are made of thin-bedded black siliceous siltstone, meter-scale intercalations of black siltstone and quartzite, massive quartzite, grey to black ribbon chert, and dolostones, respectively (4a–4c). Bartolini *et al.* (1995) and Poole *et al.* (1995) report Middle and Late Ordovician (Caradocian and Asghillian) graptolites from the “transitional unit”. A “calk-silicate siltstone unit” occurs in a fault bounded block in the central-western part of the area. White siltstones of this unit contain epidote nodules (Figure 4e) and intercalated quartz-pebble conglomerate. This unit is tentatively correlated with the Barranca Group. A unit made of andesite flows and tuffs unconformably overlies previous units (4d), which is named here “lower volcanic unit” and is lithologically correlated with the Tarahumara Formation. The previous units are intruded by different igneous bodies that caused widespread contact metamorphism. The older intrusions are coarse-grained and granitic in composition, commonly with biotite, but some facies have muscovite. Microgranite porphyry intrudes and includes xenoliths of the coarse-grained granite (4f). This porphyry is made of phenocrysts of plagioclase and quartz surrounded by white to clear-grey microcrystalline matrix. Field relationships and fabric indicate the microgranite is a hypabyssal intrusion. In turn, the porphyry is intruded

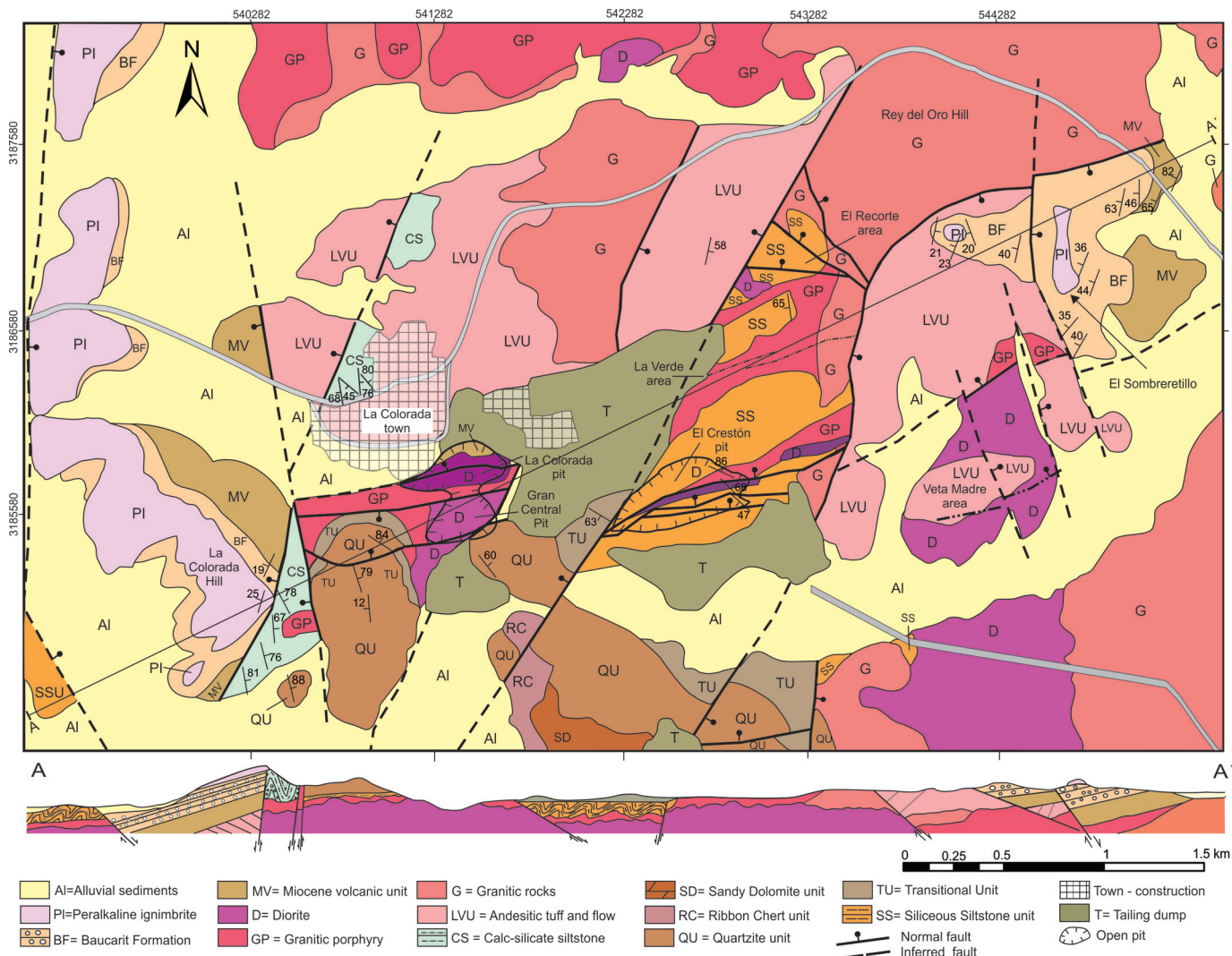


Figure 2. Geologic map of the study area and schematic section. ERF: El Recorte Fault; GCF: Gran Central fault; LCF: La Colorada fault; LAF: Las Amarillas fault; LVF: La Verde fault; NVF: North vein fault; ROF: Rey del Oro fault; SVF: South vein fault.

by medium-grained diorite to quartz-diorite, composed by amphibole and plagioclase with minor quartz and biotite. The diorite is emplaced below the microgranite along an irregular contact exposed in the Gran Central and La Colorada pits (Figure 4f). The diorite from these pits yielded three consistent $^{40}\text{Ar}/^{39}\text{Ar}$ biotite ages of 70 Ma (Zawada *et al.*, 2001) that are interpreted as a cooling age after the diorite intrusion.

Volcanic and sedimentary rocks are exposed inside fault-bounded basins (Figure 4g). The lower part is mainly made by porphyritic andesite flows with hornblende and/or plagioclase phenocrysts, which is here informally named the “Miocene volcanic unit”. Hydrothermal alteration is scarce and metamorphism absent in this unit. A correlative amphibole-bearing lava collected 4 km south of the La Colorada town yielded a 24 Ma K-Ar age (McDowell *et al.*, 2001). Based on its lithology and age, this unit may be correlated with the Oligocene-Early Miocene SCORBA event that accompanied and followed the Sierra Madre Occidental ignimbrite flare-up.

A unit made by sedimentary breccias, conglomerate, and minor tuff (Figure 4g and 4h), covers the Miocene volcanic unit. Clasts in breccias mainly derive from the underlying unit. The sedimentary sequence is capped by a ~30 m thick peralkaline rhyolite ignimbrite (Figure 4g;

Vidal-Solano *et al.*, 2008), which yielded a 12.3 Ma K-Ar age (McDowell *et al.*, 2001). The ignimbrite is part of a huge pyroclastic eruption that covered part of the Baja California and Sonora states (Vidal-Solano *et al.*, 2005; 2007; 2013; and references therein).

Mineralization

Mineralization in the La Colorada district mainly occurs along veins, splitting veinlets, and tension gashes. Host rocks are Paleozoic metasediments and the Upper Cretaceous plutonic and volcanic rocks. Veins are all fault controlled, with faulting preceding the veining. Veinlets are developed along breccia zones, anastomosing fractures, and tension joints, all of them related with faulting. McMillan *et al.* (2009) indicate that the veins commonly flared upwards into stockwork zones, and are commonly displaced a few meters by post-ore faults. Three samples from veins in the La Colorada and Gran Central pits yield $^{40}\text{Ar}/^{39}\text{Ar}$ sericite ages of 27 Ma, 24 Ma, and 22 Ma (Zawada *et al.*, 2001).

According to Zawada *et al.* (2001), intrusive rocks exhibit a low degree of competence and host much broader zones of fracture veining and silicification. This results in typically continuous low-grade zones of ore adjacent to high-grade veins. The sedimentary units

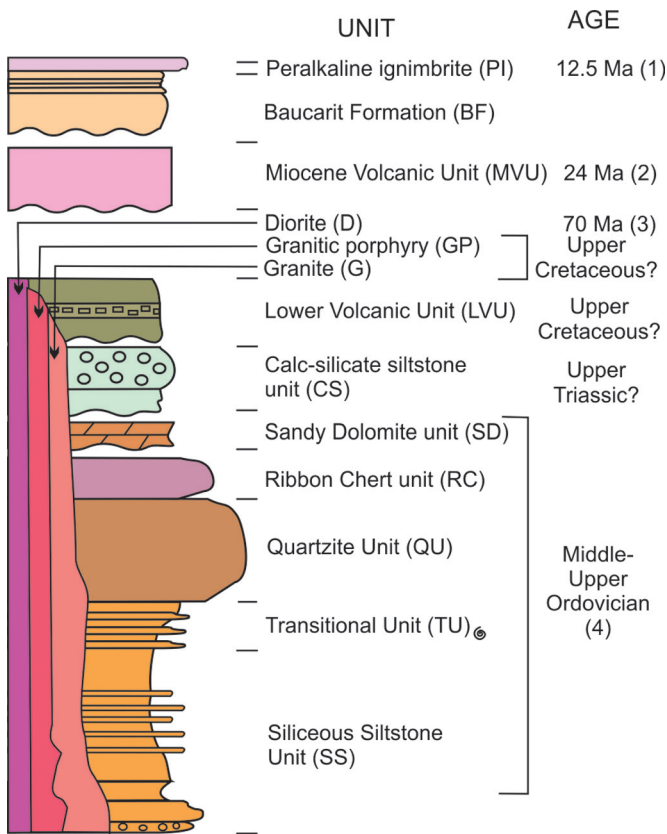


Figure 3. Stratigraphic column (1) McDowell *et al.* (1997); (2) McDowell *et al.* (2001); (3) Zawada *et al.* (2001); (4) Bartolini *et al.* (1995); Poole *et al.* (1988). Spiral indicates fossils.

generally display a higher degree of competency with more restricted quartz-filled fractures in close proximity to the veins. Historically mining was focused on high-grade veins, along which deep shafts and large adits were excavated. Veins are of microcrystalline quartz, although prismatic crystals occur in vein cavities and tension joints. Besides quartz, potassium feldspar and carbonated minerals as calcite, ankerite, and dolomite, occur. The ore consists of gold and silver, which in the El Crestón deposit have an average Au/Ag ratio of 1 to 37 (Zawada *et al.*, 2001). Veins under the oxidation zone include galena, pyrite, chalcopyrite, sphalerite, argentite, molybdenite and perhaps tetrahedrite (Ball, 1911), which are believed to have constituted less than 2% of the vein. Near surface, veins and host rocks are more oxidized displaying a maroon to ochre color. Supergene alteration yields iron and manganese oxides, argentite, malachite, azurite, chrysocolla, cerussite, as well as enrichment of native gold and silver (Zawada *et al.*, 2001). Silicification and potassic alteration consisting of quartz, K-feldspar, and sericite, are found adjacent to veins; while propylitic alteration made of sericite, clay, chlorite, epidote, and carbonate minerals, is found more distally.

METHODOLOGY

The aim of this work is to study the geological structures in the area, in particular those related with the mineralization, as well as the analysis and interpretation of these structures. In order to reach these goals, the strike, dip, and location of each fault was obtained, as well

as the pitch of slickenside lineation where present. Shear sense was defined with kinematic indicators such as displacement of markers, tectoglyphs, tension veins, and Riedel fractures. In addition to structural data, crosscutting relationships and mineralization-alteration occurrence were described in each fault. Data were plotted and analyzed with the Stereonet 8 software (Allmendinger *et al.*, 2012), while definition of the stress ellipsoid was estimated from the model of faulting of Anderson (1951), and with the Win-Tensor software of Delvaux and Sperner (2003) and the Faultkin software of Allmendinger *et al.* (2012).

STRUCTURAL GEOLOGY

Folding

Older structures in the area are folds of the Paleozoic metasediments and the “siliceous siltstone unit”. Mesoscopic folds are visible locally along the Hermosillo-Yecora highway and roads inside the mine area (Figure 5). Folds can be classified as open to tight, based on the interlimb angle; some are overturned folds with NE vergence based on the axial plane attitude. The stratification strikes mainly N50-60°W with dips both to NE and SW (Figure 6). Attitude of the Pi-axis obtained with the stereonet software is N39°W/28° (trend/plunge) and the mean axial plane attitude is S37°E 85°SW. Zawada *et al.* (2001) report inverted strata in the Paleozoic sequence that can be related to large-scale overturned folds in these rocks.

Faulting

The most common structures in the study area are normal faults. A total of 370 faults were measured throughout the area and grouped in six zones in order to perform a detailed structural analysis. These zones are: 1) Gran Central pit; 2) La Colorada pit; 3) El Crestón pit; 4) La Verde area; 5) El Recorte range; and 6) Eastern zone (Figure 2).

Gran Central pit

In this pit, diorite intrudes the microgranite porphyry along an irregular contact (Figure 7a). To the west, the diorite also intrudes quartzite and pelitic hornfels. The main structure in this pit is the Gran Central fault (Figure 8a), which was mined by ~700 m along the strike and ~330 m depth, according to an old unpublished map and section. The fault strikes ~N80°E and dip ~60° N, and the slickenside striations have a pitch of 85°N. The main fault and at least five secondary subparallel faults were target of the open cut mining. West of the Gran Central pit, the main fault juxtaposes a diorite of the footwall against Paleozoic metasediments of the hanging wall. In the eastern side of the pit the fault juxtaposes Paleozoic metasediments of the footwall against andesitic flows of the Miocene volcanic unit in the hanging wall. This fault zone is made of anastomosing fractures filled with cataclasite, Fe-oxides and gouge. Most of the structures in this area are normal faults, with relatively steep dips, although some are clearly listric. The faults displace the contact between the diorite and the microgranite porphyry, which is a clear but non-planar marker. The total displacement of the Gran Central fault cannot be quantified but may be several tens of meters, while in secondary faults the displacement is in the order of meter or less.

La Colorada pit

Along the pit wall, diorite intrudes the microgranite porphyry. La Colorada fault is the main structure in this pit, which strikes N75°E and dips ~50° NW (Figure 7b). The main fault zone includes about 20 m of anastomosing fractures with fault breccia, cataclasite, and gouge, as well as thin quartz veinlets and extensive oxidation. In the

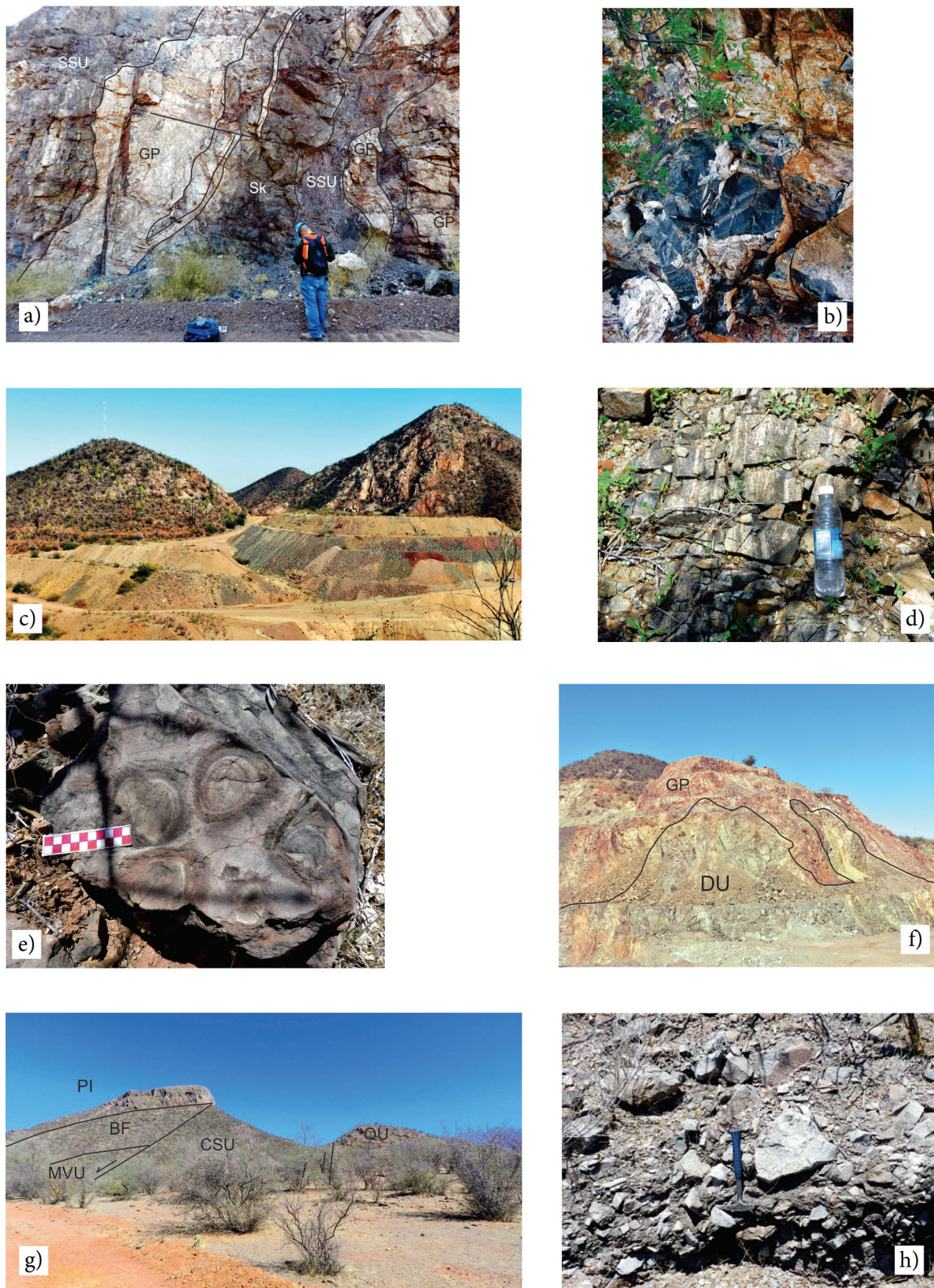


Figure 4. a) Exposure in the El Crestón pit (view to E); b) Dark siltstones of the transitional unit, Las Amarillas hill; c) Panoramic view of hills made of the Quartzite unit (view to E); d) Exposure of the Lower Volcanic unit; e) Epidote nodules of the calc-silicate siltstone unit; f) Exposure between the Gran Central and El Crestón pits (view to E); g) Panoramic view of the La Colorada hill (view to N); h) Sedimentary breccia of the Baucarit Formation. BF = Baucarit Formation; CSU = Calc-silicate unit; D = Diorite; GP = Granite Porphyry; MVU = Miocene volcanic unit; PI = Peralkaline Igneimbrite; QU = Quartzite unit; SK = Skarn; SSU = Siliceous Siltstone unit.

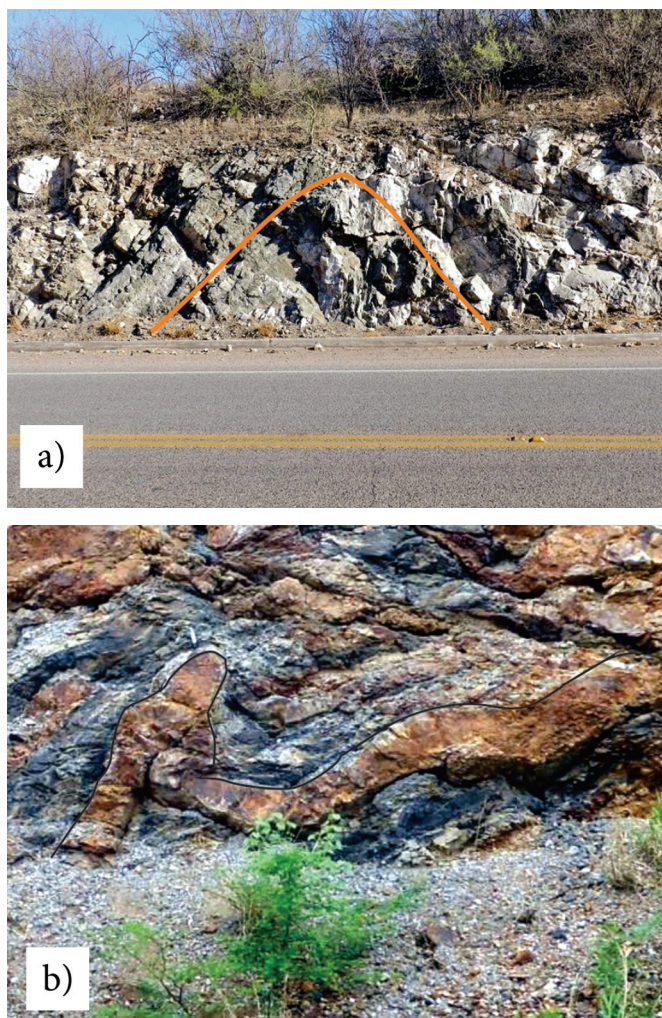


Figure 5. a) Open fold in the Calc-silicate Siltstone unit (view to N); b) Close folds in the Transitional unit (view to NW).

eastern side, the fault places andesitic rocks of the Miocene volcanic unit in the hanging wall against diorite and microdiorite in the footwall. Old underground adits followed this structure for ~ 580 m along strike, although the present pit has only 370 m of length. Drill holes by Eldorado Exploration found the mineralization about 200 m down-dip under the actual pit bottom (McMillan *et al.*, 2009).

El Crestón pit

Geology in this pit is complex including different lithologies of the Paleozoic metasediments that are intruded by dikes and apophyses of coarse-grained granitic rocks, which are displaced by a set of normal faults (Figure 7c and 8b). Contact metamorphism-metasomatism transformed the sedimentary rocks into fine-grained hornfels and local garnet-epidote skarn. Main veins strike $\sim N70^\circ E$ with dips between 70° to $50^\circ N$. Old mining adits extended ~ 580 m along the strike and the shafts reach about 260 m depth. According to Ball (1911) the veins converged upwards creating a wide zone of stockwork, which allowed mining by "open cut methods". The present open pit has a surface length of about 800 m along the vein strike, is 366 m wide, and ~ 100 m deep. At least, five large veins can be seen in the northeastern wall, each one hosting subparallel quartz veinlets with oxidation (Figure 8b).

La Verde Mine zone

According to Ball (1911) the Verde Mine was the first gold mine in the La Colorada District. Anastomosing quartz veins with pyrite and copper carbonates outcrop along 2 to 8 m width and ~ 100 m length. Old adits in this zone extended about 230 m along the strike. The main mineralized structure is the La Verde vein, with an average width of 2.4 m. This vein strikes $N75^\circ E$ and dips $70^\circ N$. Host rocks are micro-granite porphyry, granite and siliceous siltstones.

El Recorte range

This range is a fault bounded horst mainly consisting of coarse-grained granitic rocks. To the north, a NE striking normal fault juxtaposes the granite and Paleozoic metasedimentary rocks against the Upper Cretaceous (?) "Lower volcanic unit". To the south, an ENE striking fault juxtaposes the granite against Upper Cretaceous (?) volcanics, as well as with the Baucarit Formation and its cap made of the peralkaline ignimbrite. Numerous quartz veinlets, subparallel to the south boundary fault, occur in the south slope but have not been mined.

Eastern zone

This zone is located south of the El Recorte range and east of the normal fault that juxtaposes Paleozoic metasediments in the east against the Lower Volcanic unit in the west. The Upper Cretaceous dioritic intrusive is also exposed in this block. Tertiary volcanic and sedimentary rocks cover the Lower Volcanic unit.

Structural analysis

Structural data of faults in the six studied zones are displayed as pole to fault stereogram, statistical contours, and rose diagrams in Figure 9. In order to separate different populations of faults, distribution of the fault azimuths is displayed as a frequency histogram in Figure 10, which also includes a Kernel density estimation (Zucchini, 2003), both using the Excel program. In the Kernel plot, troughs occur in $\sim N51^\circ E$, $N54^\circ W$, $N25^\circ W$, and $N15^\circ E$ (Figure 10), separating four fault sets, each one consisting of two families of conjugate faults.

The main set in all zones strikes between $N51^\circ$ - $90^\circ E$ and $N54^\circ$ - $90^\circ W$ with peak at $\sim N88^\circ E$ (Figure 9, 10, and 11A, Table A of the electronic appendix). Strikes between $N51^\circ$ - $90^\circ E$ predominate in the Gran Central and El Crestón areas; while strikes between $N54^\circ$ - $90^\circ W$ predominate in the La Colorada, La Verde, and El Recorte areas (Figure 9). Faults of this group are the main host of the mineralization. This group is represented for 196 faults, 40 of which dip to the south (SE-SW) and the rest to the north (NE-NW), forming a conjugate fault system (Figure 11a). Distribution of fault poles along the N-S axis indicates the listric character of faults in this set, which was also observed in

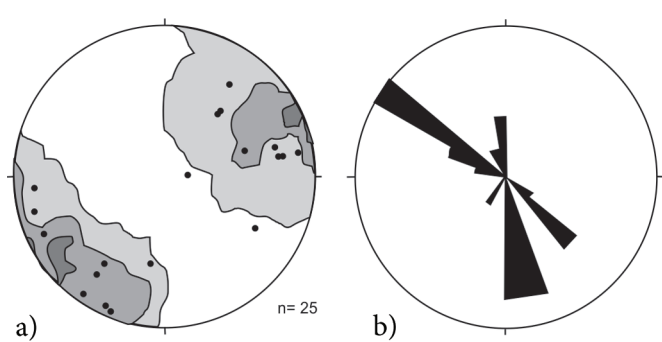


Figure 6. a) Kamb contouring of poles to stratification (lower hemisphere, equal area projection); b) Rose diagram of the strikes of stratification (right-handed rule).

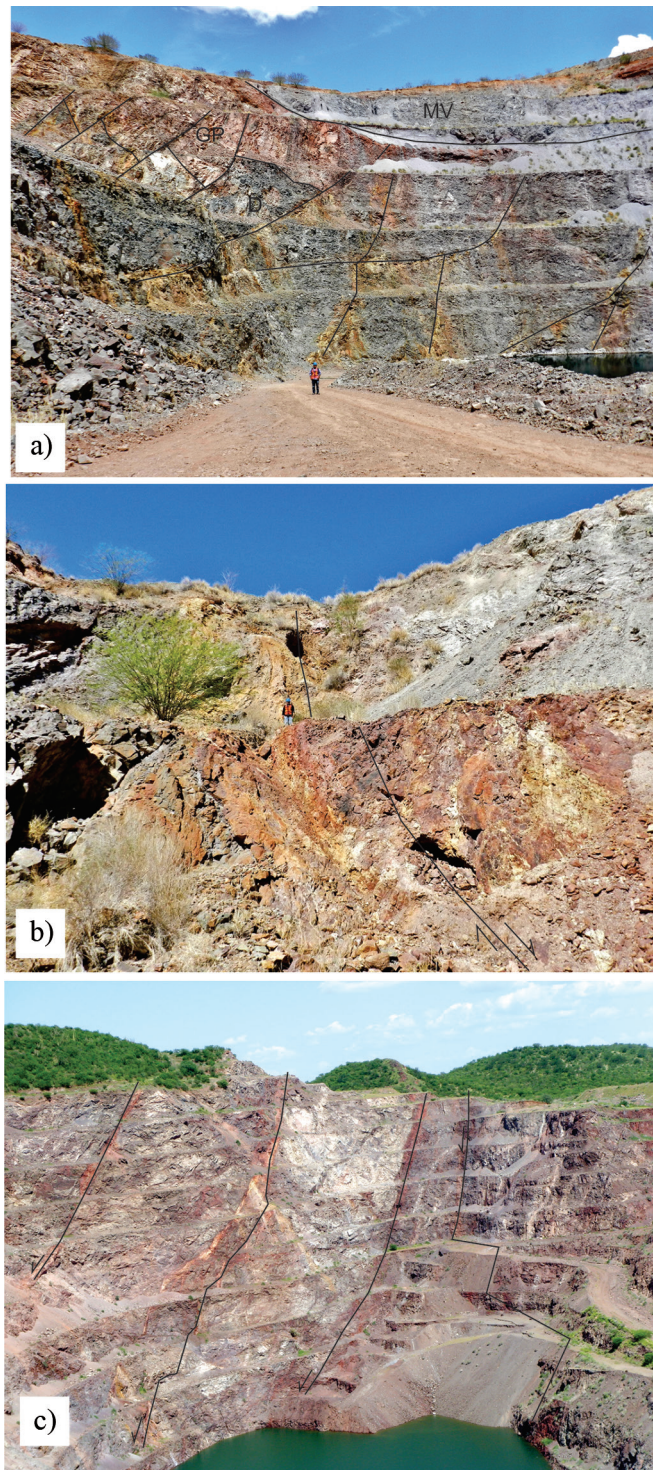


Figure 7. Panoramic view of: a) Gran Central pit (view to E); b) La Colorada pit (view to W); c) El Crestón pit (view to ENE). Main faults are highlighted. GP= Microgranite Porphyry, D= Diorite, MV= Miocene Volcanic unit.

exposures. The second fault set strikes between $N25^{\circ}$ - $54^{\circ}W$ with an average of $N40^{\circ}W$. This group is represented by 67 faults 15 dipping to the SW and the rest to the NE yielding a conjugate fault system (Figures 9, 10, and 11b). The third group of faults strikes between $N15^{\circ}$ - $51^{\circ}E$ with an average of $N34^{\circ}E$ (Figures 9, 10, and 11c). This

group includes 49 faults, 26 dipping to the SE and the rest to the NW yielding a conjugate fault system. The fourth fault set strikes between $N25^{\circ}W$ and $N15^{\circ}E$ with a mean at $N3^{\circ}W$ (Figures 9, 10 and 11d). This group encompasses 52 faults, 22 dipping to the E and the rest to the W, yielding a conjugate fault system.

The inferred relative age of the different fault sets is as follow: the ~E-W fault set is the oldest in the area, followed by the NW-SE fault set, then the NE-SW set, and finally the ~N-S set. The criteria used for the definition of the relative age are: a) direct observation of crosscutting relationships between faults of different sets (e.g. Figure 8c, Table A electronic appendix), which is also noted in the geologic map; for example, the NE-SW fault located east of the El Crestón pit and the La Verde area (Figure 2) crosscut all the mineralized ENE-WSW fault veins. Besides, neither the Miocene volcanic or sedimentary units are cut by this set or contain mineralized ores; b) the main mineralized event postdate the ENE-WSW fault set conforming the main ore bodies in the area, and predate the NW-SE, NE-SW and N-S sets; c) Miocene clastic sediments are mainly deposited along NW-SE fault basins as occurred with the Baucarit Formation in central Sonora (e.g. Bartolini *et al.*, 1994; McDowell *et al.*, 1997; Gans, 1997); d) a NE-SW normal fault limits and predates the Middle Miocene (12.3 Ma) peralkaline ignimbrite in the La Colorada hill (Figure 2); e) the ~N-S set tilt the peralkaline ignimbrite being the younger in the study area.

Dynamic analysis

Dynamic analysis seeks to define the stress field in a region following the model of faulting by Anderson (1951), which is based on the assumption that in the shallow crust one principal stress is always vertical. For normal faults the main stress σ_1 is vertical while σ_2 and σ_3 stresses are horizontal. Theoretically, a population of normal faults occurs as two families, each one dips steeply in a direction opposite to those in the other family, with σ_1 bisecting the acute angle between faults, σ_2 located parallel to the intersection line of the two faults, and σ_3 bisecting the obtuse angle between faults (see Angelier, 1994; Rowland *et al.*, 2007; Célérrier *et al.*, 2012). In the study area, the first fault set (F1) has a mean strike value of $N88^{\circ}E$ (Figure 11a, Table A), then the extension direction must be ~ $N2^{\circ}W$. The second fault set (F2) has an average strike of $N40^{\circ}W$ (Figure 11b), and then extension direction must be $N50^{\circ}E$. The third fault set (F3) has a mean strike of $N34^{\circ}E$ (Figure 11c), and then extension direction must be ~ $N56^{\circ}W$. The fourth fault set (F4) has an average strike of $N3^{\circ}W$ (Figure 11d), and the extension direction must be $N87^{\circ}E$. In the Anderson's model, if slickenside lineations are developed on a conjugate normal fault system, they must be mostly dip-directed. However, if a subsequent stress field occurs in a region, the old faults are often reactivated typically with an oblique-slip movement (Rowland *et al.*, 2007), because strain compatibility may control the slip directions of different fault sets during the later phases of deformation (Marrett and Allmendinger, 1990). Dynamic analysis does not account for possible tilting of former faults caused by latter faulting phases, which can variably modify the attitude of faults and then, the original extension directions. In order to obtain the original extension directions, tilting caused by each subsequent fault phase must be eliminated in each fault, which is impractical or unworkable.

Kinematic analysis

The model of faulting by Anderson (1951) assumes that the stress field causing deformation in the shallow crust is uniform over a large area, and then, that multiple fault types require multiple deformation episodes. However, nonuniform stress fields may occur during a single tectonic episode originating different types of faults with diverse orientations simultaneously (e.g. Molnar and Tapponnier, 1975; Reches, 1978; Marret and Allmendinger, 1990; Nieto-Samaniego and Alaniz-

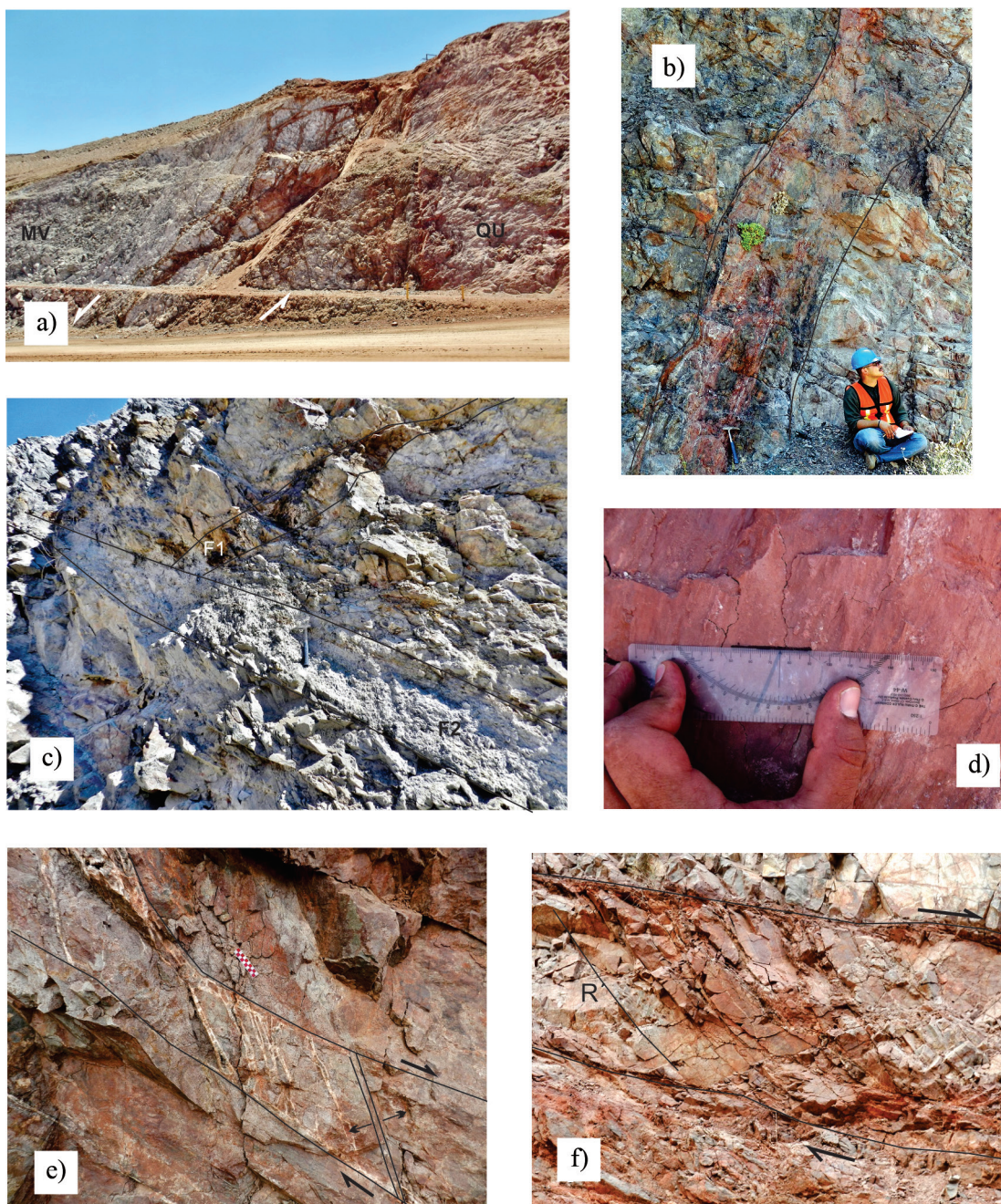


Figure 8. Some aspects of faults in the study area. a) Normal fault that juxtaposes the Quartzite unit against the Miocene Volcanic unit (view to E); b) Mineralized vein along a normal fault in the El Crestón pit (view to ENE); c) Crosscutting faults in the La Colorada pit, a mineralized NE striking fault (F1) is displaced by a non-mineralized-brecciated NW striking fault (F2) (view to N); d) Slickenside lineations with oblique displacement along a normal fault near to the Gran Central pit; e) Mineralized tension gashes between two low-angle normal faults, Gran Central pit (view to W); f) Riedel fractures (R) in a normal fault zone (view to W).

Alvarez, 1997). Kinematic analysis is a technique for analyzing fault data (e.g. Marrett and Allmendinger, 1990), which permits define the overall strain pattern in an area as well as testing for kinematic compatibility of faults sets. This analysis can only be performed in faults with slickenside lineation and definite shear sense; in the study area, 26 faults fulfill these requirements (Figure 12, Table 1). With regard to the number of faults, Arlegui-Crespo and Simón-Gómez (1998) argue that some methods produce very stable standard solutions from fault samples made up of about 25-30 faults. Inversion of fault data of the

study area was done with the FaultKin software by Allmendinger *et al.* (2012) and the Win-Tensor software by Delvaux and Sperner (2003). For analysis, fault data were separate in the four sets defined above, considering that, as indicated by Célérrier *et al.* (2012), establishing the chronological order of faulting is the first and most important step in dealing with polyphase data, which can efficiently guide the sorting process. Faults, slickenlines, and movement directions are displayed in Figure 12a.

Plot of the extension (T), shortening (P), and intermediate (B)

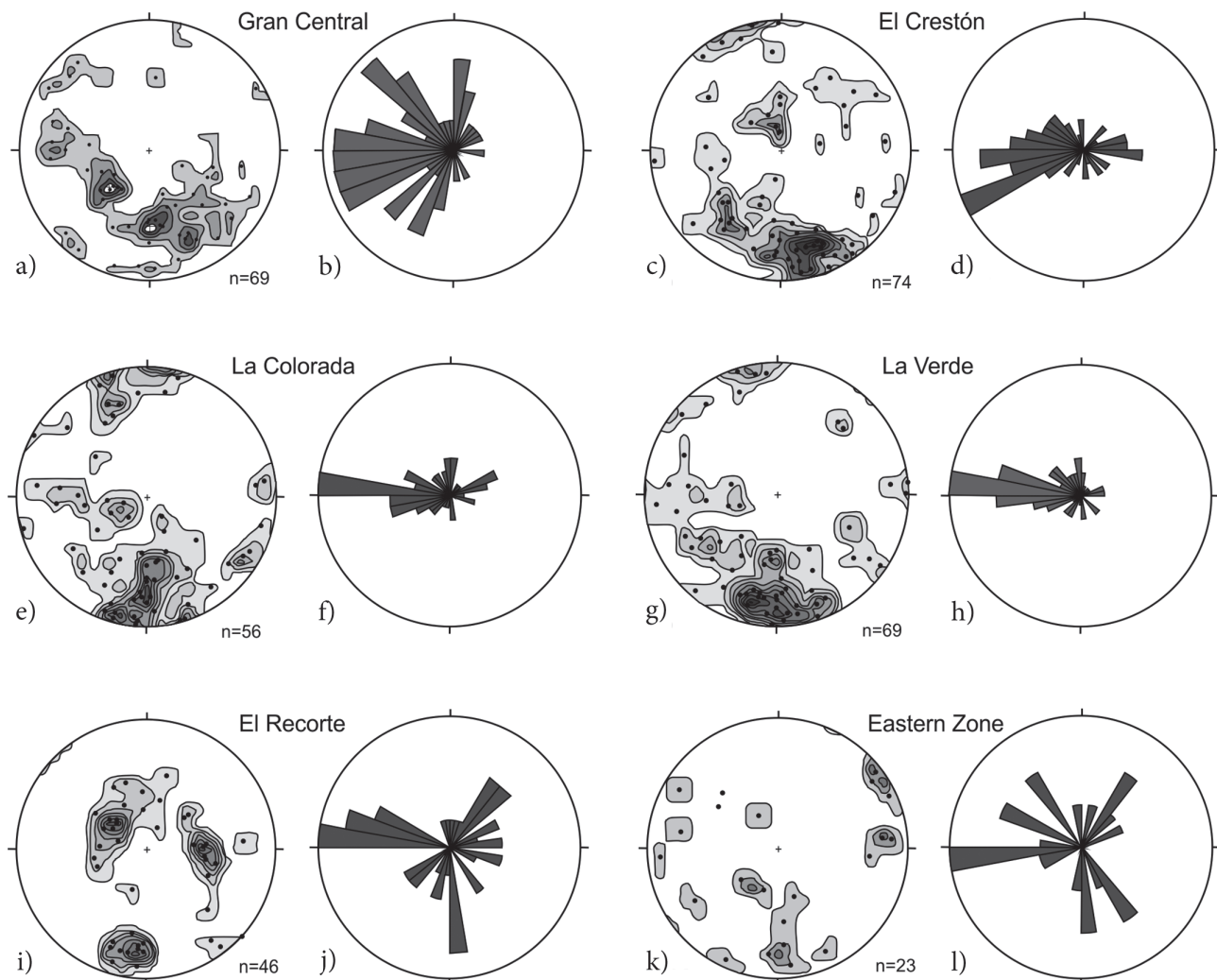


Figure 9. Lower hemisphere, equal area projections of poles to fault planes with statistical contours and rose diagram of the fault azimuths (right-handed rule). a-b) Gran Central pit and nearby areas; c-d) El Crestón pit and nearby areas; e-f) La Colorada pit; g-h) La Verde area; i-j) El Recorte area; r-l) Eastern Zone.

axes of the four fault sets is displayed in Figure 12b. Extensional axes contouring with Kamb method yield two clear groups one WNW-ESE and other NNE-SSE (Figure 12c). Most of the shortening axes make a wide E-W girdle (Figure 12d). Two fault sets are compatible if the respective extension and shortening axes coincide. In this sense, faults of the first set are kinematically incompatible with faults of the other three sets, while faults of the fourth set are compatible with faults of the third set, and partially compatible with faults of the second set.

Marret and Allmendinger (1990) indicate that kinematically heterogeneous faulting, represented by girdle or multi-modal patterns of shortening and/or extension axes, can be produced by triaxial deformation, anisotropy reactivation, strain compatibility or multi-phase deformations. A criterion supporting multiple deformations is that a single fault set displays widely varying slip directions, as in the case of F1 in the area (Figure 12a). Slip direction of F1 has highly variable slip directions, while slip directions of F4 are mostly coherent; indicating that the F1 has been reactivated whereas F4 has not been. Additional evidence for multiple deformations in the area is systematic cross-cutting relationships between fault sets (Table A) and mutually exclusive chronologic constraints on the fault sets, which have been

explained above. However, kinematic compatibility exists mainly between the third and fourth sets (Figure 12b) suggesting that they can be generated by a similar stress field.

DISCUSSION AND TECTONIC MODEL

By the end of the Mesozoic Era, the Laramide orogeny folded, faulted, and locally foliated Upper Cretaceous sedimentary and volcanic sequences (González-León *et al.*, 1992; García-Barragán and Jaques-Ayala, 2011). Folds related with this phase have NNW-SSE axis and NE vergence (González-León *et al.*, 1992), similar to those in the study area, which fold the “calk-silicate siltstone unit”.

The lower volcanic unit, granite and diorite intrusions, and the Miocene volcanic unit are all related to subduction of the Farallon plate along the western margin of the North American plate (e.g. Damon *et al.*, 1983; Roldán-Quintana, 1991; Valencia-Moreno *et al.*, 2006). Continued subduction resulted in the oblique interaction of the East Pacific Rise (EPR) with the North American plate. Transform faults fragmented the EPR causing diachronic arrival of the ridge to the

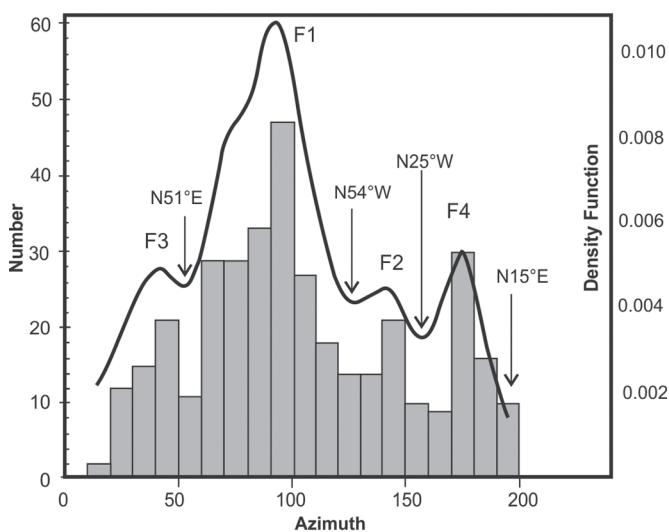


Figure 10. Frequency histogram of the fault plane azimuths, the azimuth range was selected to encompass all sets in the area (F1 to F4). The black line is a Kernel density estimation function with an H parameter of 8 (Zucchini, 2003); troughs indicate the limit between different populations. Number of faults = 369.

trench. According to Atwater and Stock (1998) and Wilson *et al.* (2005) the EPR arrived at the trench offshore southwestern California by 28.5 Ma. This arrival coincides with ages of extension in Arizona and Sonora (e.g. Cameron *et al.*, 1989; Armstrong, 1990; Dickinson, 1990; Miranda-Gasca and De Jong, 1992; Gans, 1997; Wong and Gans, 2008). The first extensional phase produced normal faults striking ~E-W. Some of these faults display dip-parallel slickenside lineations (Figure 13a). Dynamic and kinematic analysis indicates that F1 was caused by a ~vertical σ_1 , and a σ_3 striking ~N-S (Figures 11a, 12e and 12i). Similar direction of extension has not been mentioned, although Gans (1997) mention ENE-WSW strike-slip faults in the Santa Rosa region that he regards as accommodation faults related to NW-SE normal faults, which were active between 26 and 20 Ma. Similar E-W mineralized structures occur in the San Dimas District (Tayoltita, Durango), where

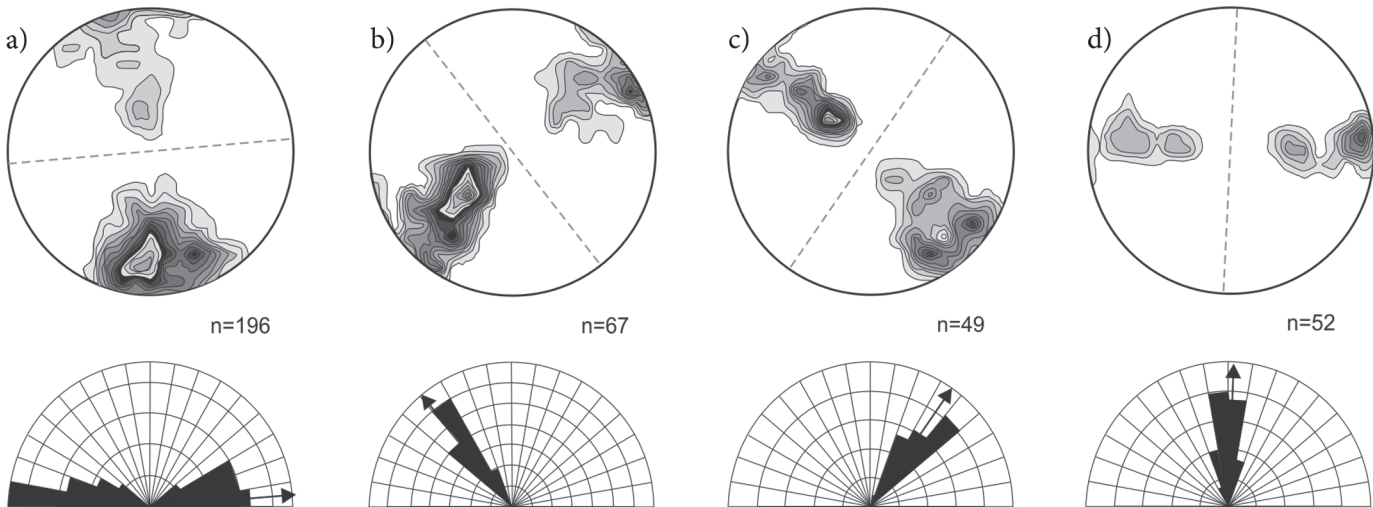


Figure 11. a to b: Statistical 1% area contours of the poles to fault planes of the four sets, lower hemisphere, equal-area projection. Segmented line indicates the average strike of each group. Below each stereogram the rose diagram displays the cumulate number of faults by azimuth; arrow indicates the average strike of each set of faults.

the veins are hosted in rocks dated between 40 and 36 Ma, and precede rocks dated between 25-20 Ma (Horner and Enríquez, 1999). These authors regard the veins as tension gashes associated with an E-W striking σ_1 and ~N-S striking σ_3 , derived from the latest compression stages of the Laramide Orogeny. Ferrari *et al.* (2007) suggest that the San Dimas veins and other mineralized veins (e.g. Staude and Barton, 2001) could be generated during a deformation phase occurring between the Laramide Orogeny and the Oligocene-Miocene extension, which these authors name “pre-Oligocene deformation”. In Nayarit, similarly oriented structures are considered as predating a 23 Ma dike (Duque-Trujillo *et al.*, 2014). Considering the Late Oligocene-Early Miocene (27-22 Ma) ages obtained in sericite of the La Colorada mineralized veins (Zawada *et al.*, 2001), the F1 set may be accommodation zones as those of the Santa Rosa region, or reactivation of older (Late Triassic?) structures as those proposed by Stewart and Roldán-Quintana (1991). Alternatively, the F1 set could be generated by intrusion of a laccolithic diorite body, which would produce a local strain. However, faults in the mine area postdate the diorite, and faulting related to shallow intrusions commonly displays a concentric or radial pattern (e.g. Cole *et al.*, 2005; Acocella *et al.*, 2000), which is not observed in the study area.

The second extensional phase produced NW-SE striking faults (F2) similar to those of the Basin and Range Province of Sonora (Figures 11b and 13e). Kinematic analysis indicates the F2 faults were originated by NE60-80°SW directed extension (Figure 12f). The same direction of extension characterizes the MCCs of Sonora and Arizona (e.g. Dickinson, 1991; Nourse *et al.*, 1994; Gans, 1997; McDowell *et al.*, 1997; Vega-Granillo and Calmus, 2003). The F2 faults may reactivate the F1 faults, generating oblique slickenside lineations on the latter (Figure 13a, 13b). This extensional event has been related to gravitational instability caused by thickened crust combined with a high geothermal gradient related with the Eocene-Oligocene magmatism (e.g. Liu and Shen, 1998; Calmus *et al.*, 2011). The age of the main extensional phase in the Mazatlán MCC is constrained between 25 and 16 Ma (Wong and Gans, 2008); while in the Santa Rosa region, is constrained to between ~26 and 20 Ma (Gans, 1997). In both, the MCC and the Basin and Range basins, volcanic rocks dated at ~27 Ma (Miranda-Gasca and De Jong, 1992; McDowell *et al.*, 1997; Gans, 1997) underlies the clastic rocks, which support a Late Oligocene inception of this extensional phase. Ferrari *et al.* (2013) and Murray *et al.* (2013) found a similar

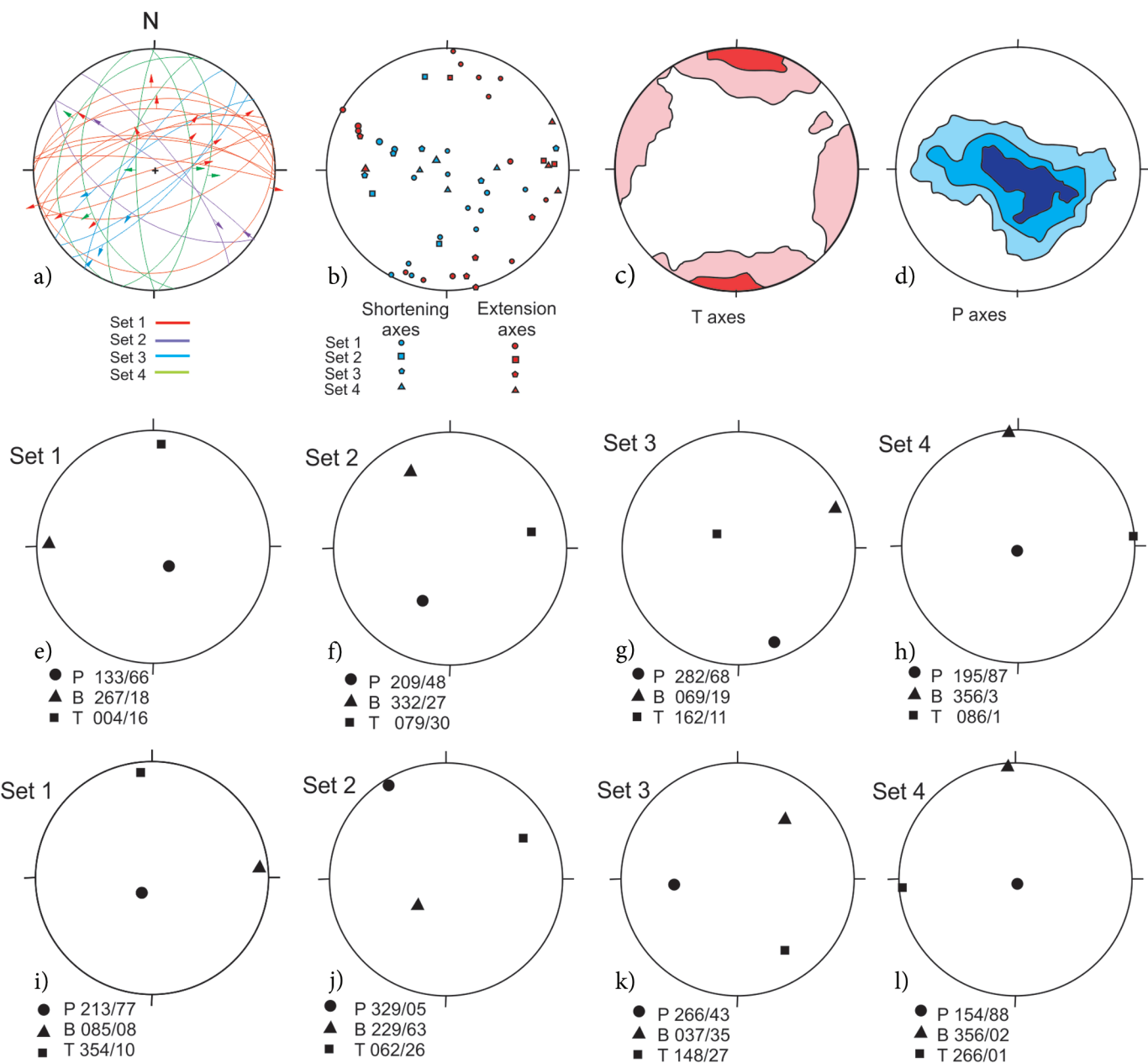


Figure 12. Results of the inversion of fault data with slickenside lineations with the Faultkin software (Marrett and Allmendinger, 1990; Allmendinger *et al.*, 2012). a) Faults with striae and slip direction; b) Shortening and extension axes; c) Kamb contours of extensional (T) axes; d) Kamb contours of the shortening (P) axes; e to h) Kinematic axes for the different fault sets calculated with the Linked Bingham distribution statistics Faultkin software (Allmendinger *et al.*, 2012); i to l) Kinematic axes obtained from the inversion of fault data with the Win-Tensor software (Delvaux and Sperner, 2003). In figures e to l circle indicates the shortening axes (P); square indicates the extension axes (T), and the triangle indicates the intermediate axes (B).

extensional phase in Sinaloa-Nayarit and in the border of Chihuahua-Sonora, respectively. Andesitic volcanism of 24 Ma (McDowell *et al.*, 2001) is coeval to the second extensional phase and may be related to the thermal source that produced the main hydrothermal event in the area, which flowed along the F1 faults generating the most important mineralized veins.

The third extensional phase originated faults striking N15°-51°E (Figure 11c). Pole to fault clusters (Figure 11) indicate that NW dipping faults are steep, while SE dipping faults have low-angle dips, which can be caused by rotation of this family during the fourth extensional phase. No dip-parallel slickenside lineations were observed in this set,

maybe due to the nature of the faults, which are formed by anastomosing, brecciated, cataclastic zones, and gouge. However, faults of the F1 and F2 sets must be reactivated during this phase generating NE and SW trending lineations (Figure 12a, Figure 13c and 13f). According to the kinematic analysis, this phase may be originated by NW-SE shortening direction (Figure 12g) or by NW-SE extension direction (Figure 12k). These apparently contradictory results can be explained by the activation of a transtensional regime with $\sigma_1 \sim N25^\circ W$ similar to the present main stress in the San Andreas-Gulf of California system, which also produces local field stress with NW-SE extension in relief zones. As discussed above the NE-SW faulting must be slightly older

Table 1. Faults with slickenside lineations

Strike	Dip	Dip direction	Pitch	Shear sense	Trend	Plunge	Plungedirection	Group
73	62	163	45°SW	normal	228	39	228	1
260	42	350	55°SW	normal	307	33	307	1
67	81	157	20°SW	right lateral	244	20	244	1
253	90	343	0	left lateral	253	0	253	1
235	75	325	46°SW	normal	250	44	250	1
250	59	340	20°NE	right lateral	59	17	59	1
245	67	335	90	normal	335	67	335	1
80	15	170	20°NE	left lateral	99	5	99	1
268	33	358	90	normal	358	33	358	1
272	49	362	90	normal	2	49	2	1
273	70	3	70°NE	normal	50	62	50	1
275	83	5	60°NE	normal	83	59	83	1
255	65	345	60°NE	normal	39	52	39	1
275	68	5	55°NE	normal	67	49	67	1
305	85	395	45°NW	normal	310	45	310	2
125	57	215	0	right lateral	125	0	125	2
322	75	52	38°SE	right lateral	131	36	131	2
51	75	141	60°SW	normal	207	57	207	3
43	72	133	26°SW	right lateral	214	25	214	3
205	23	295	83°N	normal	303	23	302.6	3
215	75	305	0	right lateral	215	0	215	3
200	68	290	90	normal	290	68	290	3
170	40	260	70°SE	normal	235	37	235	4
15	54	105	85°N	normal	97	54	97	4
358	64	88	90	normal	88	64	88	4
180	78	270	90	normal	270	78	270	4

than, or coeval with the emplacement of peralkaline ignimbrite at 12.3 Ma. Faults striking ~N35°E have been scarcely described in Sonora, although a similarly orientated system is the Empalme graben (Roldán-Quintana *et al.*, 2004). Based on chemical correlations and geological relationships of the peralkaline ignimbrite, Vidal-Solano *et al.* (2013) propose that dextral faults between Bahía Kino and the Sierra Libre displaced crustal blocks to the NW during a period of strong tectonic activity related to a proto-Gulf transtensional episode. Then, the stress responsible for the displacement of the Gulf of California, can originally be active over a large area of Sonora and Baja California, creating the Gulf Extensional Province of Karig and Jensky (1972), which is considered to have been active sometime between ~12 and 6 Ma (e.g. Henry and Aranda-Gómez, 2000; Bennett *et al.*, 2013; Bennett and Oskin, 2014). A stress field with a ~N25°W oriented σ_1 and ~N65°E oriented σ_3 , may have produced dextral strike-slip faults striking ~N55°W, parallel to the present Gulf Fault System, as well as normal faults striking ~N35°E in relief zones, as those in the pull-apart basins of the Gulf of California.

The fourth extensional phase originated conjugate normal fault system (F4) striking ~N-S, with dip-parallel slickenside lineations (Figure 12a, Figure 13j). This phase reactivate previous fault sets producing ~E-W trending slickenside lineations (Figure 12a; Figure 13d, 13g, 13i). Kinematic analysis indicates this phase was produced by ~E-W extension with ~vertical shortening direction (Figure 12h, 12l). Faults with similar orientation displacing NW-SE oriented faults have been described in many localities of Sonora (e.g. Gans, 1997). In the MCC of Sonora, late N-S faults create basins along which clastic sediments overlie older Tertiary strata in angular unconformity (e.g. Miranda-Gasca and De Jong, 1992; Vega-Granillo and Calmus, 2003).

We proposed that the NNW-SSE faults in the coastal and inner region of Sonora may have been caused by a permutation of σ_2 by σ_1 , which occurred ~6 Ma ago once the transtensional regime was released from the continent and concentrated in the Gulf of California fault system (Bennett *et al.*, 2013; Bennett and Oskin, 2014).

CONCLUSION

Detailed structural study in the La Colorado mine area indicates a complex tectonic history since the Late Cretaceous. Rocks intruded by a Late Cretaceous (~70 Ma) diorite body are affected by a folding phase related to the Laramide Orogeny. Four phases of normal faulting were recognized and its relative ages defined based on crosscutting relationships, rock ages, field observations, and structural analyses. Faults of the first phase strike ENE-WSW to E-W, dip to N or S, and host the main mineralized veins in the area. This phase must have occurred prior to the age of the hydrothermal event at 27-22 Ma. The inception of this phase as well as its regional tectonic significance remains to be precisely defined. The second extensional phase produced faults with NW-SE strikes and SW to NE dips, reactivating the F1 faults. We associate this phase with the formation of the Basin and Range province and the MCCs in Sonora and Arizona, between ~26 and 15 Ma ago (Dickinson, 1991; Nourse *et al.*, 1994; Gans, 1997; Vega-Granillo and Calmus, 2003; Wong and Gans, 2008). The inception of this phase coincides with the arrival of segments of the East Pacific Rise to the trench. The third extensional phase produces faults with NE-SW strike and NW or SE dips, and reactivated the F1 and F2 sets. The stress field responsible for the normal faults must have a

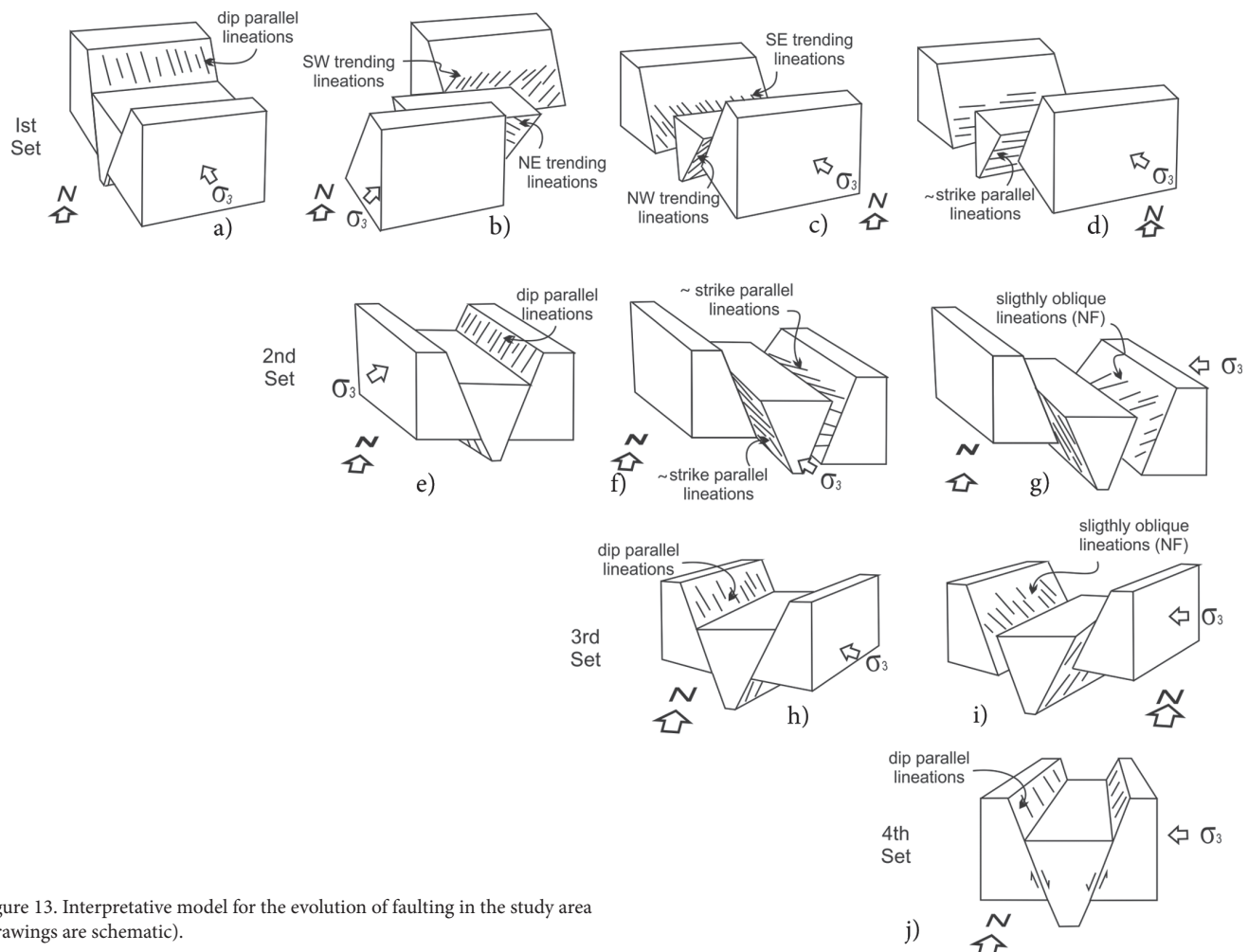


Figure 13. Interpretative model for the evolution of faulting in the study area (drawings are schematic).

~vertical σ_1 and σ_3 ~N35°W. Based on available data, we interpret that between 12.5 and 6 Ma a transtensional regime was imposed in a region including part of Sonora and Baja California, producing the Gulf Extensional Province. That regime was caused by a field stress with σ_1 ~horizontal and oriented ~N25°W and with σ_2 vertical. We infer that the NW-SE trending extension of this phase can be related with step-over between the NW-SE strike-slip faults. About 6 Ma ago, concentration of right-lateral movement in the present Gulf of California fault system may have released the ~N25°W horizontal σ_1 stress in the continent, causing a change in the field stress, which may have originated the fourth extensional phase in the area.

ACKNOWLEDGEMENT

This research was partially funded by a CONACYT (177668) grant to Ricardo Vega-Granillo and by an ARGONAUT GOLD grant to Víctor Hugo Vázquez Armenta.

REFERENCES

Acocella, V., Cifelli, F., Funiciello, R., 2000, Analogue models of collapse calderas and resurgent domes: *Journal of Volcanology and Geothermal Research* 104, 81-96.

Albrecht, A., Goldstein, S.L., 2000, Effects of basement composition and age on silicic magmas across an accreted terrane-Precambrian crust boundary, Sierra Madre Occidental, Mexico: *Journal of South American Earth Sciences*, 13, 255-273.

Alencaster de Cserna, G., 1961, *Estratigrafía del Triásico Superior de la parte norte central del estado de Sonora*: Universidad Nacional Autónoma de México, Instituto de Geología, Paleontología Mexicana No.11, Parte I, 1-18.

Allmendinger, R.W., Cardozo, N., Fisher, D., 2012, *Structural Geology Algorithms: Vectors and Tensors in Structural Geology*: Cambridge University Press, 289 pp.

Anderson, E.M., 1951, *The Dynamics of Faulting and Dyke Formations*: Edinburgh and London, Oliver & Boyd, 206 pp.

Anderson, T.H., Silver, L.T., 2005, The Mojave-Sonora megashear – field and analytical studies leading to the conception and evolution of the hypothesis: *Geological Society of America, Special paper* 393, 1-50.

Angelier, J., 1994, Fault slip analysis and paleostress reconstruction, in Hancock, P. (ed.), *Continental Deformation*: New York, Pergamon, 53-100.

Arlegui-Crespo, L.E., Simón-Gómez, J.L., 1998, Reliability of palaeostress analysis from fault striations in near multidirectional extension stress fields. Example from the Ebro Basin, Spain: *Journal of Structural Geology*, 20 (7), 827-840.

Armstrong, R.L., 1990, Cenozoic magmatism in the North American Cordillera and the origin of metamorphic core complexes: *Geological Society of America Abstracts with Programs*, 22, 4.

Atwater, T., Stock, J., 1998, Pacific-North America Plate Tectonics of the Neogene Southwestern United States - An Update, *International Geological Review*, 40, 375-402.

Ball, S.H., 1911, Geological report upon the property of the Mines Company of America, 22 pp. (unpublished).

Bartolini, C., Damon, P.E., Shafiqullah, M., Morales-Montaña, M., 1994,

Geochronologic contribution to the Tertiary sedimentary-volcanic sequences (Báucarit Formation) in Sonora, México: *Geofísica Internacional*, 33, 67-77.

Bartolini, C., Morales-Montaño, M., Barrera-Moreno, E., Domínguez-Perla, J.E., Navarro-Martínez, L.A., Soto-Contreras, L.A., Finney, S.C., Carter, C., 1995, Geologic reconnaissance of Ordovician deep-marine sequences in central Sonora, Mexico, in Cooper, J.D., Drosler, M.L., and Finney, S.C. (eds.), *Ordovician Odyssey: Short Papers for the Seventh International Symposium on the Ordovician System: Short Papers for the Seventh International Symposium on the Ordovician System*: Fullerton, Calif., Pacific Section Society for Sedimentary Geology (SEPM), book no. 77, 285-289.

Bennett, S.E.K., Oskin, M.E., 2014, Oblique rifting ruptures continents: Example from the Gulf of California shear zone: *Geology*, 42(3), 215-218.

Bennett, S.E.K., Oskin, M.E., Iriondo, A., 2013, Transtensional Rifting in the Proto-Gulf of California Near Bahía Kino, Sonora, México: *Geological Society of America Bulletin*, 125(11/12), 1752-1782.

Calmus, T., Vega-Granillo, R., Zazueta-Lugo, R., 2011, Evolución geológica de Sonora durante el Cretácico Tardío y el Cenozoico, in Calmus, T. (ed.), *Panorama de la geología de Sonora*, México: Universidad Nacional Autónoma de México, Instituto de Geología, Boletín 118(7), 227-266.

Cameron, K.L., Nimz, G.J., Kuentz, D., Niemeyer, S., Gunn, S., 1989, Southern Cordilleran basaltic andesite suite, southern Chihuahua, Mexico; a link between Tertiary continental arc and flood basalt magmatism in North America: *Journal of Geophysical Research*, 94, 7817-7840.

Célérier, B., Etchecopar, A., Bergerat, F., Vergely, P., Arthaud, F., Laurent, P., 2012, Inferring stress from faulting: From early concepts to inverse methods: *Tectonophysics* 581, 206-219.

Cole, J.W., Milner, D.M., Spinks, K.D., 2005, Calderas and caldera structures: a review, *Earth-Science Reviews* 69, 1-26.

Coney, J.P., Campa, M.F., 1984, Terrenos sospechosos de aloctonía y acreción del occidente y sur del continente norteamericano: *Boletín del Departamento de Geología Universidad de Sonora*, 1(1), 1-24.

Damon, P.E., Shafiqullah, M., Roldán-Quintana, J., Cochemé, J.J., 1983, El batolito Laramide (90-40 Ma) de Sonora: XV Convención Nacional de la Asociación de Ingenieros de Minas, Metalurgistas y Geólogos de México, Guadalajara, Jalisco, México, 63-95.

Delvaux, D., Sperner, B., 2003, Stress tensor inversion from fault kinematic indicators and focal mechanism data: the TENSOR program, in Nieuwland, D. (ed.), *New Insights into Structural Interpretation and Modelling*, Geological Society, London, Special Publications 212, 75-100.

Dickinson, W.R., 1991, Tectonic setting of faulted Tertiary strata associated with the Catalina core complex in southern Arizona: *Geological Society of America, Special Paper* 264, 1-106.

Duque-Trujillo, J., Ferrari, L., Norini, G., López-Martínez, M., 2014, Miocene faulting in the southwestern Sierra Madre Occidental, Nayarit, Mexico: kinematics and segmentation during the initial rifting of the southern Gulf of California, *Revista Mexicana de Ciencias Geológicas*, 31(3), 283-302.

Ferrari, L., Valencia-Moreno, M., Bryan, S., 2007, Magmatism and tectonics of the Sierra Madre Occidental and its relation with the evolution of the western margin of North America: *Geological Society of America Special Paper* 422, 1-39.

Ferrari, L., López-Martínez, M., Orozco-Esquivel, T., Bryan, S.E., Duque-Trujillo, J., Lonsdale, P., Solari, L., 2013, Late Oligocene to Middle Miocene rifting and synextensional magmatism in the southwestern Sierra Madre Occidental, Mexico: The beginning of the Gulf of California rift: *Geosphere*, 9 (5), 1161-1200.

Gans, P.B., 1997, Large-magnitude Oligo-Miocene extension in southern Sonora: Implications for the tectonic evolution of northwest Mexico: *Tectonics*, 16, 388-408.

García-Barragán, J.C., Jacques-Ayala, C., 2011, Estratigrafía del Cretácico de Sonora, México, in Calmus, T. (ed.), *Panorama de la geología de Sonora*, México: Universidad Nacional Autónoma de México, Instituto de Geología, Boletín 118(5), 113-199.

González-León, C.M., Roldán-Quintana, J., Rodríguez-Guerra, E.P., 1992, Deformaciones Sevier y Laramide – su presencia en Sonora: Universidad de Sonora, Boletín del Departamento de Geología, 9, 1-18.

González-León, C.M., McIntosh, W.C., Lozano-Santacruz, R., Valencia-Moreno, M., Amaya-Martínez, R., Rodríguez-Castañeda, J.L., 2011, Cretaceous and Tertiary sedimentary, magmatic, and tectonic evolution in north-central Sonora (Arizpe and Bacanuchi Quadrangles), northwest Mexico, *Geological Society of America Bulletin*, 123, 600-610.

Henry, C.D., Aranda-Gómez, J.J., 2000, Plate interactions control middle late Miocene proto-Gulf and Basin and Range extension in the southern Basin and Range: *Tectonophysics*, 318, 1-26.

Horner, J.T., Enríquez, E., 1999, Epithermal precious metal mineralization in a strike-slip corridor: the San Dimas district, Durango, Mexico: *Economic Geology*, 94, 1375-1380.

Karig, D.E., Jenks, W., 1972, The Proto-Gulf of California: *Earth and Planetary Science Letters*, 17, 169-174.

Ketner, K.B., Noll, J.H.Jr., 1987, Preliminary geologic map of the Cerro Cobachi area, Sonora, Mexico: U.S. Geological Survey Miscellaneous Field Studies Map MF-1980, scale 1:20,000.

King, R.E., 1939, Geological reconnaissance in northern Sierra Madre Occidental: *Geological Society of America Bulletin*, 50, 1625-1722.

Lewis, P.D., Taite, S.P., Bowen, B.K., Mustard, J., Zawada, R.D., Pacheco, H.R., 1995, Geological report of the La Colorada property, Sonora, Mexico: Unpublished report for Exploraciones Eldorado, S.A. de C.V., Hermosillo, Mexico, 107 pp.

Liu, M., Shen, Y., 1998, Crustal collapse, mantle upwelling, and Cenozoic extension in the North American Cordillera: *Tectonics*, 17(2), 311-321.

Marrett, R., Allmendinger, R.W., 1990, Kinematic analysis of fault-slip data: *Journal of Structural Geology*, 12(8), 973-986.

McDowell, F.W., Clabaugh, S.E., 1981, The igneous History of the Sierra Madre Occidental and its Relation to the Tectonic Evolution of Western Mexico. Universidad Nacional Autónoma de México: Instituto de Geología Revista, 5(2), 195-206.

McDowell, F.W., Keizer, R.P., 1977, Timing of mid-Tertiary volcanism in the Sierra Madre Occidental between Durango City and Mazatlán, Mexico: *Geological Society of America Bulletin*, 88, 1479-1487.

McDowell, F.W., Mauger, R.L., 1994, K-Ar and U-Pb zircon chronology of Late Cretaceous and Tertiary magmatism in central Chihuahua State, Mexico: *Geological Society of America Bulletin*, 106, 118-132.

McDowell, F.W., Roldán-Quintana, J., Amaya-Martínez, R., 1997, Interrelationship of sedimentary and volcanic deposits associated with Tertiary extension in Sonora, Mexico: *Bulletin of the Geological Society of America*, 109, 1349-1360.

McDowell, F.W., Roldán-Quintana, J., Connelly, J.N., 2001, Duration of Late Cretaceous-early Tertiary magmatism in east-central Sonora, Mexico: *Geological Society of America Bulletin*, 113, 521-531.

McMillan, R.H., Hodder, S., 2008, Technical Report on the Corona Gold-Silver Property, Sierra Madre Occidental, State of Chihuahua, Mexico for Comstock Metals Ltd. Report # 917, A.C.A. Howe International Limited, Toronto, Ontario, Canada, 81 pp.

McMillan, R.H., Dawson, J.M., Giroux, G.H., 2009, Geologic Report on the La Colorada Property with a resource Estimate on La Colorada and El Crestón Mineralized Zones, Sonora Mexico, prepared for Pediment Gold Corp, November 30, 2009, 141 pp.

Miranda-Gasca, M.A., De Jong, K.A., 1992, The Magdalena mid-Tertiary extensional basin, in Clark, K.F.; Roldán-Quintana, J. and Schmidt, R.H. (eds.), *Geology and mineral resources of northern Sierra Madre Occidental*, Mexico: The El Paso Geological Society, Guidebook for the 1992 Field Conference, 377-384.

Molnar, P., Tapponnier, P., 1975, Cenozoic tectonics of Asia: Effects of a continental collision: *Science*, 189, 419-426.

Mora-Álvarez, G., McDowell, F.W., 2000, Miocene volcanism during late Subduction and early rifting in the Sierra Santa Ursula of western Sonora, Mexico, in Delgado-Granados, H., Aguirre-Díaz, G., Stock, J.M. (eds.), *Cenozoic tectonics and volcanism of Mexico*: Boulder, Colorado, Geological Society of America Special Paper 334, 123-141.

Murray, B.P., Busby, C.J., Ferrari, L., Solari, L., 2013, Synvolcanic crustal extension during the mid-Cenozoic ignimbrite flare-up in the northern Sierra Madre Occidental, Mexico: Evidence from the Guazapares Mining District region, western Chihuahua, *Geosphere*, 9 (5), 1201-1235.

Nieto-Samaniego, A.F., Alaniz-Alvarez, S.A., 1997, Origin and tectonic interpretation of multiple fault patterns: *Tectonophysics* 270, 197-206.

Nourse, J.A., Anderson, T.H., Silver, L.T., 1994, Tertiary metamorphic core complexes in Sonora, northwestern Mexico: *Tectonics*, 13, 1161-1182.

Paz-Moreno, F., Demant, A., Cochemé, J.J., Dostal, J., Montigny, R., 2003, The Quaternary Moctezuma volcanic field—A tholeiitic to alkali basaltic episode in the central Sonoran Basin and Range Province, México, in Johnson, S.E., Paterson, S.R., Fletcher, J.M., Girty, G.H., Kimbrough, D.L., Martín-Barajas, A. (eds.), Tectonic evolution of northwestern Mexico and the southwestern USA: Geological Society of America Special Paper 374, 439-455.

Poole, F.G., Madrid, R.J., 1988, Allochthonous Paleozoic eugeoclinal rocks of the Barita de Sonora mine area, central Sonora, Mexico, in Rodríguez-Torres, R., (ed.), El Paleozoico de la región central del Estado de Sonora: Libreto Guía de la Excursión para el segundo simposio sobre la geología y minería en el Estado de Sonora. Instituto de Geología, UNAM, 32-41.

Poole, F.G., Madrid, R.J., Morales-Ramirez, J.M., 1988, Paleozoic eugeoclinal rocks of the Sonoran orogen in the Barita de Sonora mine area, central Sonora, Mexico [abs.], in Almazán-Vázquez, E., Fernández-Aguirre, M.A. (eds.), Resúmenes, Segundo Simposio sobre Geología y Minería de Sonora: Hermosillo, Sonora, Mexico, Universidad Nacional Autónoma de México, Instituto de Geología, 50-51.

Poole, F.G., Stewart, J.H., Berry, W.B.N., Harris, A.G., Repetski, J.E., Madrid, R.J., Ketner, K.B., Carter, C., Morales-Ramirez, J.M., 1995, Ordovician ocean-basin rocks of Sonora, Mexico, in Cooper, J.D., Drosler, M.L., Finney, S.C. (eds.), Ordovician Odyssey: Short Papers for the Seventh International Symposium on the Ordovician System, Las Vegas: Fullerton, California, Pacific Section Society for Sedimentary Geology (SEPM), book no. 77, 277-284.

Radelli, L., Menicucci, S., Mesnier, H., Calmus, T., Amaya-Martinez, R., Barrera, E., Domínguez, E., Navarro, L., Soto, L., 1987, Allochthonous Paleozoic bodies of Central Sonora: Boletín del Departamento de Geología, Universidad de Sonora, 4, 1-15.

Ramos-Velázquez, E., Calmus T., Valencia V., Iriondo A., Valencia-Moreno M., Bellon H., 2008, Laramide coastal Sonora batholith, U-Pb and $^{40}\text{Ar}/^{39}\text{Ar}$ geochronology of the coastal Sonora batholith: New insights on Laramide continental arc magmatism: Revista Mexicana de Ciencias Geológicas, 25(2), 314-333.

Reches, Z., 1978, Analysis of faulting in three-dimensional strain field: Tectonophysics 47, 109-129.

Roldán-Quintana, J., 1991, Geology and chemical composition of El Jaralito and Aconchi batholiths, in east-central Sonora, in Pérez-Segura, E., Jacques-Ayala, C. (eds.), Studies of Sonoran geology: Geological Society of America, Special Paper, 254, 69-80.

Roldán-Quintana, J., Mora-Klepeis, G., Calmus, T., Valencia-Moreno, M., Lozano-Santacruz, R., 2004, El graben de Empalme, Sonora, México: magmatismo y tectónica extensional asociados a la ruptura inicial del Golfo de California: Revista Mexicana de Ciencias Geológicas, 21, 320-334.

Rowland, S.M., Duebendorfer, E.M., Schifelbein, I.M., 2007, Structural Analysis and Synthesis a laboratory course in Structural Geology (third edition): Oxford, Blackwell publishing, 301 pp.

Staude, J.M., Barton, M.D., 2001, Jurassic to Holocene tectonics, magmatism, and metallogeny of northwestern Mexico: Geological Society of America Bulletin, 113, 1357-1374.

Stewart, J.H., Roldán-Quintana, J., 1991, Upper Triassic Barranca Group; Nonmarine and shallow-marine rift-basin deposits of northwestern Mexico, in Pérez-Segura, E., Jacques-Ayala, C. (eds.), Studies of Sonoran geology: Geological Society of America, Special Paper, 254, 19-36.

Stewart, J.H., McMenamin, M.A.S., Morales-Ramirez, J.M., 1984, Upper Proterozoic and Cambrian rocks in the Cabo Corral region, Sonora, Mexico—Physical stratigraphy, biostratigraphy, paleocurrent studies, and regional relations: U.S. Geological Survey Professional Paper 1309, 36 pp.

Valencia-Moreno, M., Ruiz, J., Barton, M.D., Patchett, P.J., Zürcher, L., Hodkinson, D., Roldán-Quintana, J., 2001, A chemical and isotopic study of the Laramide granitic belt of northwestern Mexico—identification of the southern edge of the North American Precambrian basement: Geological Society of America Bulletin, 113, 1409-1422.

Valencia-Moreno, M., Iriondo, A., González-León, C.M., 2006, New $^{40}\text{Ar}/^{39}\text{Ar}$ hornblende dates of granitic rocks from central Sonora, NW Mexico—a systematic study of crystallization age during east migration of the Late Cretaceous-early Tertiary magmatic activity: Journal of South American Earth Sciences, 22, 22-38.

Vega-Granillo, R., Calmus, T., 2003, Mazatán metamorphic core complex (Sonora, Mexico) - Structures along the detachment fault and its exhumation evolution, Journal of South American Earth Sciences, 16(4), 193-204.

Vidal-Solano, J.R., Paz-Moreno, F.A., Iriondo, A., Demant, A., Cochemé, J.J., 2005, Middle Miocene peralkaline ignimbrites in the Hermosillo region (Sonora, México). Geodynamic implications: Comptes Rendus Geoscience, 337, 1421-1430.

Vidal-Solano, J.R., Paz-Moreno, F.A., Demant, A., López-Martínez, M., 2007, Ignimbritas hiperacalinas del Mioceno medio en Sonora Central: reevaluación de la estratigrafía y significado del volcanismo terciario, Revista Mexicana de Ciencias Geológicas, 24(1), 47-67.

Vidal-Solano, J.R., Lapierre, H., Stock, J.M., Demant, A., Paz-Moreno, F.A., Bosch, D., Brunet, P., Amortegui, A., 2008, Isotope geochemistry and petrogenesis of peralkaline Middle Miocene ignimbrites from central Sonora: relationship with continental break-up and the birth of the Gulf of California, Bulletin Société Géologique du France, 179(5), 453-464.

Vidal-Solano, J.R., Lozano-Santa Cruz, R., Zamora, O., Mendoza-Cordova, A., Stock, J.M., 2013, Geochemistry of the extensive peralkaline pyroclastic flow deposit of NW Mexico, based on conventional and handheld X-ray fluorescence. Geochemical and Tectonic Implications in a regional context: Journal of Iberian Geology, 39(1), 121-130.

Weber, R., 1995, A new species of Scoresbya Harris and Sonoraphyllum gen. nov. (Plantae Incertae sedis) from the Late Triassic of Sonora, Mexico: Revista Mexicana de Ciencias Geológicas, 12, 68-93.

Weber, R., Zambrano-García, A., Amozurrutia-Silva, F., 1980, Nuevas contribuciones al conocimiento de la taifoflora de la Formación Santa Clara (Triásico Tardío) de Sonora: Universidad Nacional Autónoma de México: Instituto de Geología, Revista, 4, 125-137.

Wilson, D.S., McCrory, P.A., Stanley, R.G., 2005, Implications of volcanism in coastal California for the Neogene deformation history of western North America: Tectonics, 24, 1-22.

Wong, M.S., Gans, P.B., 2008, Geologic, structural, and thermo-chronologic constraints on the tectonic evolution of the Sierra Mazatán core complex, Sonora, Mexico—New insights into metamorphic core complex formation: Tectonics, 27, 1-31.

Zawada, R.D., 1998, La Colorada Gold Mine Sonora, Mexico, in Clark, K.F. (ed.), Gold Deposits of Northern Sonora, Mexico, Society of Economic Geologist Guidebook Series, 30, 87-99.

Zawada, R.D., Albinson, T., Aneyta, R., 2001, Geology of the El Creston Gold Deposit, Sonora State, Mexico, Economic Geology Special Publication #8, New Mines and Discoveries in Mexico and Central America, 187-197.

Zucchini, W., 2003, Applied Smoothing Techniques, Part 1: Kernel Density Estimation. <<http://staff.ustc.edu.cn/~zwp/teach/Math-Stat/kernel.pdf>

Manuscript received: January 20, 2015

Corrected manuscript received: March 5, 2015

Manuscript accepted: March 7, 2015